International Journal of Materials and Chemistry 2015, 5(4): 91-95
DOI: 10.5923/j.ijmc.20150504.02

# Properties of Sol-Gel Coated Fibers of Polyamide 6/12/ Polyvinylpyrrolidone/Nanodiamond

**Ayesha Kausar**

Nanosciences and Catalysis Division, National Centre For Physics, Quaid-i-Azam University Campus, Islamabad, Pakistan

**Abstract** In this paper, sol-gel coated and non-coated fibers of polyamide 6/12 (PA6/12) have been reported. Four type of fibers were fabricated i.e. PA6/12 and nanodiamond-based PA6/12/ND; PA6/12, polyvinylpyrrolidone and nanodiamond-based PA6/12/PVP/ND; sol-gel coated s-PA6/12/ND; and s-PA6/12/PVP/ND. The fibers were formed using a Brabender single screw extruder at 200°C. The fibers were coated using simple dip-coating technique. The structural characterization was performed using FTIR. The fractured surface of non-coated fibers was smooth without any particulate matter, while s-PA6/12/ND, and s-PA6/12/PVP/ND had some traces of sol-gel particles. However all fibers were uniformly aligned. Glass transition temperature of the sol gel fibers increased up to 271°C (s-PA6/12/PVP/ND). The sol-gel coated s-PA6/12/PVP/ND (7.5%) fibers had higher water absorbing tendency than non-coated PA6/12/PVP/ND (7.3 %).

**Keywords** Polyamide, Fiber, Nanodiamond, Sol-gel

## 1. Introduction

Aramid fibers are a category of strongly synthetic and heat-resilient fibers [1]. In such fibers, the chain molecules are greatly positioned alongside the fiber axis, hence the strength of the chemical bonding can be maneuvered. For the first time, aromatic polyamides were instigated in commercial requisitions in early 1960s, with a meta-aramid fiber designed by DuPont as Nomex [2, 3]. This fiber, which administers similar to ordinary textile wear fibers, is described by its exceptional heat resistance, as it neither melts down nor erupts under regular oxygen levels. It is extensively used in the manufacture of protective air filtration, apparel, electrical, and thermal insulation as well as an alternative to asbestos. Aramid fibers are being employed progressively in a broad spectrum of applications owing to their high specific strength, high modulus, low density, and high thermal resilience of aramid. In 2002, world production capacity of *para*-aramid was calculated as around 41,000 tonnes per year and it is increasing by an amount of 5-10% each year [4]. In 2007, this resourced an overall production capacity of about 55,000 tonnes per year. Aramids are usually manufactured through reaction between the amine group and carboxylic acid halide group [5, 6]. After the polymer production, the aramid fiber is formed by blending the liquefied polymer to solid fiber by liquid chemical blend. For the purpose of spinning, polymer solvent is normally 100% anhydrous sulfuric acid ($H_2SO_4$). Besides *meta* and *para*-aramid, additional variations are associated to the range of aramid fiber. These are principally of the copolyamide kind, best identified under the brand label Technora, as established by Teijin and familiarized in 1976. The engineering procedure of Technora presents the reaction of *p*-phenylene diamine and 3,4'-diaminodiphenylether with terephthaloyl chloride [7]. Such relatively simple procedure consumes merely single amide solvent, and hence spinning can be performed directly after the polymer formation. The long-standing service in harsh environment is desired when employed in space and aviation engineering. The features of aramid fiber mark it appropriate for countless industries. It can be present in cables, optical fiber, ballistics, linear tension members, conveyer and transmission belts, tires, as well as cut and heat protection [8]. Owed to its less stiffness, density and high resilience to destruction, it is extensively utilized in the transportation and marine industries to construct stronger, stiffer, lighter, and many more long-lasting parts [9]. Oxide or oxide-based coatings have been layered on several substrate resources through sol-gel methods [10, 11]. There are numerous potential gains of sol-gel procedure for preparing aramid fibers with photo-shielded coating films such as less expense in both the precursors and the coating equipment, low pressure and low temperature processing circumstances, fast output and no destruction to the substrate resources. Additionally the large area films can be simply manufactured during the course of processing, because the sol-gel route is a liquid-phase procedure. Employing the sol-gel technique to modify these 3D structures encounters two imperative

* Corresponding author:
asheesgreat@yahoo.com (Ayesha Kausar)
Published online at http://journal.sapub.org/ijmc

conditions *(i)* the process proceeds in liquid environment and ranges all the sections of the 3D substrate confirming complete surface coating of the substrate; *(ii)* reasonably low pressure (atmospheric pressure) and temperature (room temperature) in all the stages inhibit thermal degradation of the 3D structure [12-14]. Researchers have also reformed the physical and thermal features of polymer fibers by composite system manufacture [15-17]. Nanodiamond (ND) formed by detonation production are based on uniform and small particles of ~5 nm in diameter and signifies an accessible and huge surface area. Bulky diamond has numerous matchless characteristics comprising superior stiffness, thermal conductivity, Young's modulus, hardness, high refraction index, and a high resistivity [18]. There are numerous research efforts addressing the thermoplastics reinforcement with ND. Even without surface modification and at low concentrations, ND has been accounted to reinforce several thermoplastics [19, 20]. In this effort, polyamide 6/12 (PA6/12) and nanodiamond and PA6/12, polyvinylpyrrolidone and nanodiamond-based fibers have been prepared and coated using sol-gel route. The structure, morphological, thermal and water absorption characteristics of novel fibers have been investigated.

# 2. Experimental

## 2.1. Materials

Polyvinylpyrrolidone (average mol. wt. 40,000 $gmol^{-1}$), polyamide 6/12 (PA 6/12), diamond nanopowder, <10 nm particle size), tetraethyl orthosilicate (TEOS, 99.99%) and titanium (IV) butoxide (TBO, 97%) were supplied by Aldrich.

## 2.2. Characterization Techniques

IR spectra were taken at room temperature with a resolution of 4 $cm^{-1}$ using Excalibur Series FTIR Spectrometer, Model No. FTSW 300 MX manufactured by BIO-RAD. The scanning electron microscopic (SEM) images were obtained by Scanning Electron Microscope S-4700 (Japan Hitachi Co. Ltd.). Differential scanning calorimetry (DSC) was performed by a METTLER TOLEDO DSC 822 differential scanning calorimeter taking 5 mg of the samples encapsulated in aluminum pans and heated at a rate of 10°C/min under nitrogen atmosphere. Water absorption tendency of the fibers was evaluated by immersing equal weights of the sample films in water for 100 h at ambient temperature. The water uptake was calculated using Eq 1.

$$\%\ Water\ uptake \frac{w_2 - w_1}{w_1} \quad (1)$$

Where,
$w_1$- Initial membrane weight (g)
$w_2$- Final membrane weight (g)

## 2.3. Preparation of TBO Coating

10 mL of TBO was added to 10 mL of absolute ethanol with continuous stirring of 1h. Afterward, 1 mL of TEOS was added to this mixture and stirred for additional 1h. The solution was then diluted to 50 mL of absolute ethanol.

## 2.4. Preparation of Polyamide 6/12/nanodiamond (PA6/12/ND)

The polyamide 6/12 and nanodiamond were placed in a vacuum oven at 70°C for 24 h to remove any moisture content. The neat PA6/12 and nanodiamond nanocomposite fibers were prepared using a Brabender single screw extruder (Intelli-torque) and a single hole fiber die (diameter = 0.012 inches L/D ratio = 3). The temperature was kept at 200°C with a screw speed of 3 rpm. The extruded fibers were stretched with draw ratio 3 using Instron fiber clamps at room temperature. Stretched samples were used for characterization [21].

## 2.5. Preparation of Polyamide 6/12/polyvinylpyrrolidone/nanodiamond (PA6/12/PVP/ND)

The polyamide 6/12, polyvinylpyrrolidone and nanodiamond fibers were prepared using similar procedure mentioned in Section 2.4. The difference is that the desired amount of polyvinylpyrrolidone was also added along with the PA6/12. FTIR ($cm^{-1}$): 3330 (N–H stretching vibration), 2999 (C–H stretching vibration), 1663 (C=O, PVP), 1598 (N–H bending vibration).

## 2.6. Sol-gel coating of s-PA6/12/ND and s-PA6/12/PVP/ND Fibers

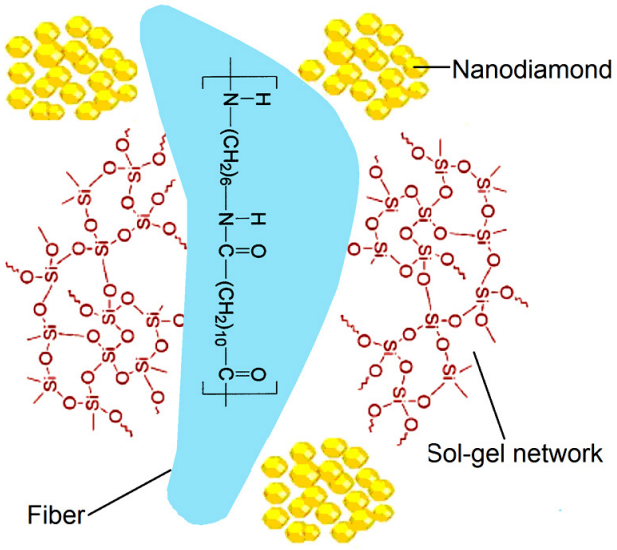


**Figure 1.** A schematic diagram for sol-gel coated s-PA6/12//ND fiber

The fibers were coated with TBO using simple dip-coating technique with a dipping rate of 100 mm $min^{-1}$. The immersion time was kept 1h for all the fibers. The number of deposited layers was 1, 5, or 10. After deposition,

the samples were washed and dried at 80°C for 24 h (Figure 1). FTIR ($cm^{-1}$): 3323 (N–H stretching vibration), 2990 (C–H stretching vibration), 1661 (C=O, PVP) 1592 (N–H bending vibration), 1024 (Si–O–Si asymmetric stretching), 922 (Si–OH), 800 (Si–O–Si symmetric stretching), 460 (Si–O–Si bending mode).

# 3. Results and Discussion

### 3.1. Microscopic Studies

The fracture surface of tested specimens was examined using SEM (Figure 2). The micrographs illustrated that the neat fibers had very smooth surface without any aggregation or particulate matter (Figure 2A). As it can be clearly seen that there is uniform alignment of the fibers prepared. Figure 2B showed that the sol-gel coated polyamide 6/12/nanodiamond fibers were uniformly oriented. However, some traces of sol-gel coating can be seen over the surface of fibers. The PA6/12/PVP/ND fibers were also uniformly aligned with smooth surface (Figure 2C). However, the same fibers with sol-gel coating were aligned with traces of particles over the fiber surface (Figure 2D). No fibers pull out phenomenon was observed on the fractured surface. In addition, the interface de-bonding, cracking, or delamination was also not experiential in sol-gel coated fibers. The occurrence of smaller particles over the surface means that the interfacial bonding between the sol-gel network and fiber was strong. This caused an increase in the mechanical properties of the composites.

### 3.2. Thermal Characterization

The nanocomposite melting was studied by performing DSC. The thermograms of PA6/12/ND, s-PA6/12/ND, PA6/12/PVP/ND and s-PA6/12/PVP/ND were recorded at heating rate of 10°C/min in $N_2$. The DSC traces of the samples were compared in Figure 3. A summary of the DSC data corresponding to the curves for the heating scan are tabulated in Table 1. The data indicated that the peaks of the sol-gel coated fibers were shifted towards right. The glass transition temperature ($T_g$) was also enhanced from 260°C in PA6/12/ND to 265°C s-PA6/12/ND. For s-PA6/12/PVP/ND, the $T_g$ was 271°C relative to s-PA6/12/PVP/ND. The obvious fact was the sol-gel network coating on polyamide fibers that caused an increase in the rigidity of nanocomposite. The silanol groups were primarily responsible for this characteristic. The incorporation of nanodiamond particles within the chain interstices also increased the overall rigidity probably by enhancing the interaction with the polyamide backbone. Analogous results have been reported in literature for polyamide/silica nanocomposites [22, 23]. In our nanocomposites, the glass transition temperature was increased by sol-gel coating.

**Table 1.** Glass transition temperature and % water uptake of sol-gel coated fibers

| Samples | $T_g$ (°C) | Water uptake (%) |
|---|---|---|
| PA6/12/ND | 260 | 6.1 |
| s-PA6/12/ND | 265 | 6.5 |
| PA6/12/PVP/ND | 269 | 7.3 |
| s-PA6/12/PVP/ND | 271 | 7.5 |

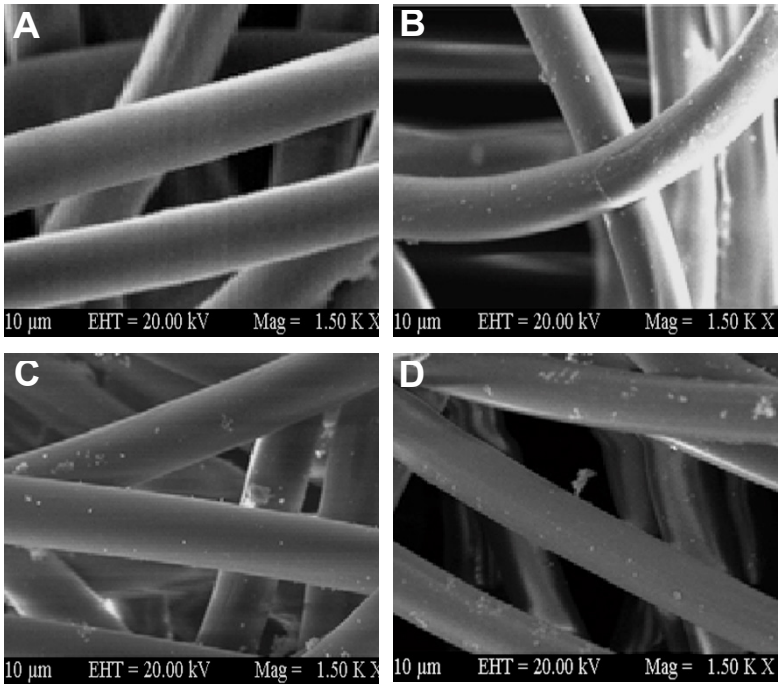


**Figure 2.** FESEM images of (A) Neat polyamide fiber; (B) s-PA6/12//ND; (C) PA6/12/PVP/ND; and (D) s-PA6/12/PVP/ND

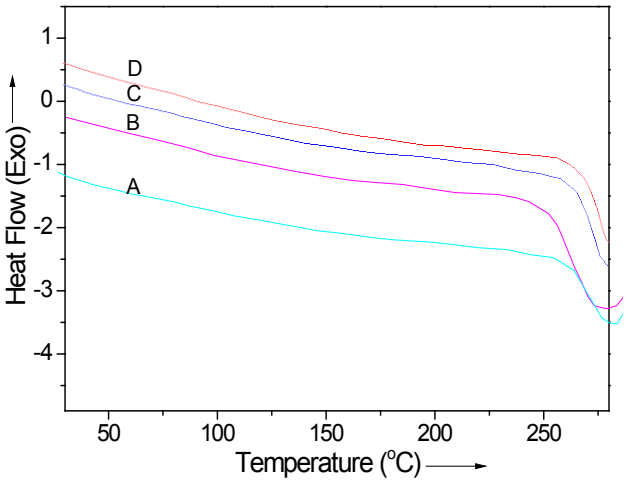


**Figure 3.** DSC thermograms of (A) PA6/12/ND; (B) s-PA6/12/ND (C) PA6/12/PVP/ND; and (D) s-PA6/12/PVP/ND at heating rate of 10 °C/min in $N_2$

### 3.3. Water Absorption Behavior

The water uptake characteristics of PA6/12/ND, s-PA6/12/ND, PA6/12/PVP/ND, and s-PA6/12/PVP/ND are depicted in Table 1. Figure 4 shows the comparative water uptake characteristics of the fibers. The structure of sol-gel coated polyamide seems to be hydrophilic and tends to absorb water easily. It was observed that the s-PA6/12/ND had water uptake of 6.5%, higher than the non-coated fiber PA6/12/ND (6.1%). The incorporation of polyvinylpyrrolidone along with the nanodiamond in the fibers render them more hydrophilic. Here again the sol-gel coated s-PA6/12/PVP/ND fibers had higher water absorbing tendency than non-coated PA6/12/PVP/ND. Correspondingly, the water uptake was increased from 7.3 to 7.5%. Thus the sol-gel fibers depicted higher water uptake compared with the other fibers. The propensity can be explained on the basis of sol-gel network formation [24, 25]. The TEOS sol-gel network structure formation led to the formation of porous structure over the fiber surface. The porous structure assisted greater water absorption compared with that of PA6/12/ND and PA6/12/PVP/ND fibers.

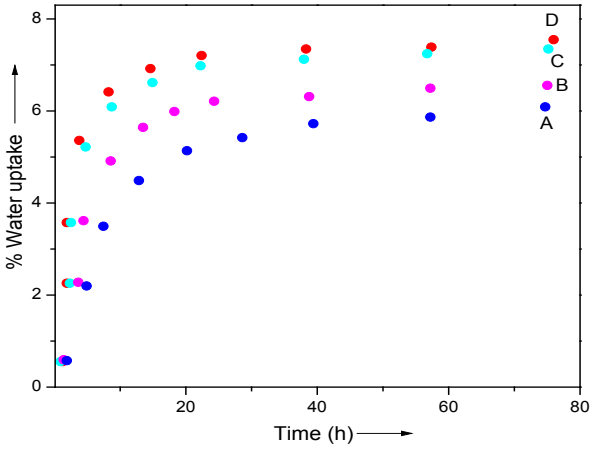


**Figure 4.** Water uptake characteristics of (A) PA6/12/ND; (B) s-PA6/12/ND (C) PA6/12/PVP/ND; and (D) s-PA6/12/PVP/ND

## 4. Conclusions

Simple and straight forward techniques were used for the preparation of polyamide 6/12 composite fibers and their sol-gel coating. In this regard, silica and nanodiamond have been introduced as low-cost inorganic and organic nanoparticles. The fibers showed remarkable physical properties so can be employed as talented material for range of technical applications. The sol-gel network on the fiber surface developed better compatibility with polyamide 6/12 containing nanodiamond and also PVP in matrix. The composite fibers depicted fine thermal performance as characterized by DSC. Morphology study revealed smooth and homogeneously aligned fiber formation. The sol-gel coated fibers also supported greater water absorption compared with the non-coated polyamide fibers.

## REFERENCES

[1] Demircan, O., Kosui, T., Ashibe, S., Nakai, A., 2014, Effect of Stitch and Biaxial Yarn Types on Tensile, Bending and Impact Properties of Biaxial Weft Knitted Composites, Adv. Compos. Mater., 23, 239-260.

[2] Foo, C. C., Chai, G. B., Seah, L. K., 2007, Mechanical properties of Nomex material and Nomex honeycomb structure. Composite Structures, 80, 588–594.

[3] Herup, E. J., Palazotto, A. N., 1998, Low-velocity impact damage initiation in graphite/epoxy/Nomex honeycomb-sandwich plates, Compos. Sci. Tech., 57, 1581–1598.

[4] Kausar A., 2014, Mechanical, Rheological and Flammability Properties of Poly(acrylonitrile-co-methyl acrylate)/Poly (3,4-ethylenedioxythiophene)/Modified Nanoclay Hybrids, Am. J. Polym. Sci., 4, 94-100.

[5] Ou, R., Zhao, H., Sui, S., Song, Y., Wang, Q., 2010, Reinforcing effects of Kevlar fiber on the mechanical properties of wood-flour/high-density-polyethylene composites, Compos. Part A Appl. Sci. Manuf., 41, 1272–1278.

[6] Kausar, A., 2014, Mechanical, thermal and electrical properties of epoxy matrix composites reinforced with polyamide-grafted-MWCNT/poly(azo-pyridine-benzopheno ne-imide)/ polyaniline nanofibers, Int. J. Polym. Mater. Polym. Biomater., 63, 831-839.

[7] Derombise, G., Schoors, L. V. V., Davies, P., 2009, Degradation of Technora aramid fibres in alkaline and neutral environments, Polym. Degrad. Stab., 94, 1615–1620.

[8] Kausar, A., 2014, Polyamide-Grafted-Multi-walled Carbon Nanotube Electrosupn Nanofibers/Epoxy Composites, Fibers Polym., 15, 2564-2571.

[9] Song, Y. S., Oh, H., Jeong, T. T., Youn, J. R., 2008, A Novel Manufacturing Method for Carbon Nanotube/Aramid Fiber Filled Hybrid Multi-component Composites, Adv. Compos. Mater., 17, 333-341.

[10] Wen, J., Wilkes, G. L., 1995, Synthesis and characterization of abrasion resistant coating materials prepared by the

sol-gel approach: I. Coatings based on functionalized aliphatic diols and diethylenetriamine, J. Inorg. Organometal Polym., 5, 343–375.

[11] Gupta, N., Sinha, T. J. M., Varma, I. K., 1997, Development of an abrasion resistant coating from organic-inorganic polymeric network by sol-gel process, Indian J. Chem. Technol. 4, 130–134.

[12] Pignatello, R., Nassar, E. J., Ciuffi, K. J., Calefi, P. S., Rocha, L. A., De Faria, E. H., Silva, M. L. A., Luz, P. P., Bandeira, L. C., Cestari, A., Fernandes, C. N., 2011, Biomaterials and sol-gel process: a methodology for the preparation of functional materials, Biomater. Sci. Eng., 2011, 1–28.

[13] Bandeira, L. C., Ciuffi, K. J., Calefi, P. S., Nassar, E. J., Salvado, I. M. M., Fernandes, M. H. F. V., 2011, Low temperature synthesis of bioactive materials, Ceraˆmica., 57, 166–72.

[14] Bandeira, L. C., Ciuffi, K. J., Calefi, P. S., Nassar, E. J., Silva, J. V. L., Oliveira, M., Maia, I. A., Salvador, I. M., Fernandes, M. H. V., 2012, Effect of a calcium phosphate coating on polyamide substrate for biomaterial applications, J. Braz. Chem. Soc., 23, 810–817.

[15] Cze´ge´ny, Z., Jakab, E., Blazso´, M., Bhaskar, T., Sakata, Y., 2012, Thermal decomposition of polymer mixtures of PVC, PET and ABS containing brominated flame retardant: formation of chlorinated and brominated organic compounds, J. Anal. Appl. Pyrol., 96, 69–77.

[16] Kausar A., 2014, Fabrication and Properties of Polyamide and Graphene Oxide Coated Carbon Fiber Reinforced Epoxy Composites, Am. J. Polym. Sci., 4, 88-93.

[17] Yang, X. F., Li, Q. L., Chen, Z. P., Zhang, L., Zhou, Y., 2013, Mechanism studies of thermolysis process in copolyamide 66 containing triaryl phosphine oxide, J. Therm. Anal. Calorim., 112, 567-571.

[18] Mochalin, V. N., Shenderova, O., Ho, D., Gogotsi, Y., 2012, The properties and applications of nanodiamonds, Nature Nanotechnol., 7, 11-23.

[19] Schmidlin, L., Pichot, V., Comet, M., Josset, S., Rabu, P., Spitzer, D., 2012, Identification, quantification and modification of detonation nanodiamond functional groups, Diam. Relat. Mater., 22, 113-117.

[20] Tomita, S., Burian, A., Dore, J. C., LeBolloch, D., Fujii, M., Hayashi, S., 2002, Diamond nanoparticles to carbon onions transformation: X-ray diffraction studies, Carbon, 40, 1469-1474.

[21] Kausar, A., Hussain, S. T., 2013, Poly(azo-ether-imide) nanocomposite films reinforced with nanofibers electrospun from multi-walled carbon nanotube filled poly(azo-ether-imide). J. Plast. Film Sheet., 30, 266-283.

[22] de Campos, B. M., Calefi, P. S., Ciuffi, K. J., de Faria, E. H., Rocha, L. A., Nassar, E. J., Silva,J. V. L., Oliveira, M. F., Maia, I. A., 2014, Coating of polyamide 12 by sol–gel methodology. J. Therm. Anal. Calorim., 115, 1029-1035.

[23] Gornicka, B., Gorecki, L., 2010, TGA/DTG/DSC investigation of thermal ageing effects on polyamide–imide enamel. J. Therm. Anal. Calorim., 101, 647-650.

[24] Jördens, C., Wietzke, S., Scheller, M., Koch. M., 2010, Investigation of the water absorption in polyamide and wood plastic composite by terahertz time-domain spectroscopy. Polym. Test., 29, 209-215.

[25] Zhang Q., Li, D., Lai, D., You, Y., Ou, B., 2015, Preparation, microstructure, mechanical, and thermal properties of in situ polymerized polyimide/organically modified sericite mica composites. Polym. Compos., DOI: 10.1002/pc.23402.